Supporting Information

Titanium carbide MXenes combine red-emitting carbon dots as a unique turn-on fluorescent probe for label-free determination of glucose

Xiaohua Zhu*, Xiao Pang, Youyu Zhang and Shouzhuo Yao

Key Laboratory of Chemical Biology and Traditional Chinese Medicine Research (Ministry of Education), College of Chemistry and Chemical Engineering, Hunan Normal University, Changsha 410081, P.R. China

*to whom corresponding should be addressed.

Tel: +86-731-88865515; Fax: +86-731-88872531

Email: zhuxiaohua@hunnu.edu.cn

Table of Content

1. **General Experimental Procedures.** **S3-S4**

2. **Supplemental Tables and Figures.** **S5-S18**

3. **References.** **S19**

Additional Experimental

Fourier transform infrared spectra (FTIR) were recorded on a Fourier transform spectrometer (TENSOR27, Bruker, Germany). The ζ-potential of different samples were determined by a Zetasizer Nano-ZS (Malvern Instruments, UK).

Detection of glucose in real samples.

The fresh human blood samples were supplied by the local hospital and obtained through venipuncture. Some necessary processes were conducted to get the serum samples and plasma samples. The blood samples without anticoagulant were rested at room temperature until blood clotted. The blood samples were centrifuged at 3000 rpm for 5 min to get serum samples. Then, all supernatant serum samples were subjected to a 10-fold dilution with PBS before analysis, and a certain concentration of glucose was added to prepare the spiked samples. The blood samples with anticoagulant ($EDTAK_2$) were centrifuged at 3000 rpm for 5 min to get plasma samples. All supernatant plasma samples and whole blood samples were subjected to a 10-fold dilution with PBS when analysis. These samples were added into GOx solution (50 μg mL^{-1}) and incubated for 1 h. Then, 500 μL DSPE-PEG/Ti_3C_2 (0.1 mg mL^{-1}) containing 5 μg RCDs aqueous solution was added into the reaction product. After incubation for 2 h at 37 °C, the fluorescence spectra of the mixture were recorded from 550 nm to 800 nm (excited at 500 nm).

Calculation of quantum yield

The quantum yield (QY) of the CDs was calculated using rhodamine B (QY = 0.56) in ethanol (η = 1.36) as the standard and 550 nm as the excitation wavelength as

reference. For calculation of quantum yield, different concentrations of each compound were made, all of which had absorbance less than 0.1 at 550 nm. The RCDs were dissolved in ethanol (η = 1.36). Their fluorescence spectra were recorded at excitation of 500 nm. Then by comparing the integrated fluorescence intensities and the absorbency values (at 500 nm) of the RCDs samples with the references rhodamine B QY of the samples were determined.

The QY was calculated according to:

$$\Phi_x = \Phi_{st} \frac{m_x}{m_{st}} \frac{\eta_x^2}{\eta_{st}^2}$$

Where Φ is the quantum yield, m is the slope of the standard (st) rhodamine B and RCDs (x), η is the refractive index of the solvent, the QY for RCDs is found to be 60.8 %.

Table S1. Comparison of the precursor, method, and quantum yield RCDs with reported in the literature.

Precursor	Method	Quantum yield (%)	Reference
2,5-Diaminobenzenesulfonic acid, 4-aminophenylboronic acid hydrochloride	hydrothermal	5.44	1
phellodendron chinense schneid	solvothermal	9.2	2
Urea, p-phenylenediamine	hydrothermal	24	3
p-phenylenediamine, HNO_3	hydrothermal	31	4
1,3-Dihydroxynaphthalene, KIO_4	solvothermal	53	5
p-phenylenediamine, KIO_4	solvothermal	>60	This work

Table S2. Comparison of the method for H_2O_2 detections in this work with some previously reported strategies.

Probe	Linear range (mM)	Detection limit (mM)	Reference
CCP/NIR CdTe/CdS QDs	0.2-4	0.1	6
BCQDs	0.1-1	--	7
Fe_3O_4@CdTe QDs	0.05-1	0.35	8
GQDs	0.1-10	0.02	9
DSPE-PEG/Ti_3C_2/RCDs	0.1-20	0.03	This work

CCP: cationic conjugated polymer; NIR: near-infrared; QDs: quantum dots; BCQDs: B-doped carbon quantum dots; GQDs: graphene quantum dots.

Table S3. Comparison of the method for glucose detections in this work with some previously reported strategies.

Probe	Linear range (mM)	Detection limit (mM)	Reference
CCP/NIR CdTe/CdS QDs	0.1	0.05	6
Au NCs@FGO	1-10	0.16	10
CdTe QDs	0.5-16	0.5	11
Au NCs@PNAS-APBA-ARS	0.5-10	0.1	12
PHPMA@PMAETMA	0.1-1	0.1	13
AgNP-CdSe QDs	2-52	1.86	14
DSPE-PEG/Ti_3C_2/RCDs	0.1-20	0.05	This work

CCP: cationic conjugated polymer; NIR: near-infrared; QDs: quantum dots; Au NCs: Gold nanoclusters; FGO: fluorescent graphene oxide; PNAS: N-acryloxysuccinimide, APBA: 3-aminophenyl boronic acid; ARS: Alizarin Red S; PHPMA: poly(N-(2-hydroxy-propyl)methacrylamide); AgNP: Ag nanoparticle.

Table S4. Amounts of glucose in human serum and whole blood samples measured with the DSPE-PEG/Ti_3C_2/RCDs nanosystem.

No.	Measured (mM)	Added (mM)	Found (mM)	Recovery (%)	RSD (%)
1	4.59	1.00	5.86	104.8	2.7
2	7.38	1.00	8.26	98.6	1.9
3	4.01	1.00	5.21	104.0	2.3
4	6.51	1.00	7.46	99.3	3.1

1. fasting plasma glucose, 2. after breakfast, 3. fasting whole blood glucose, 4. after breakfast.

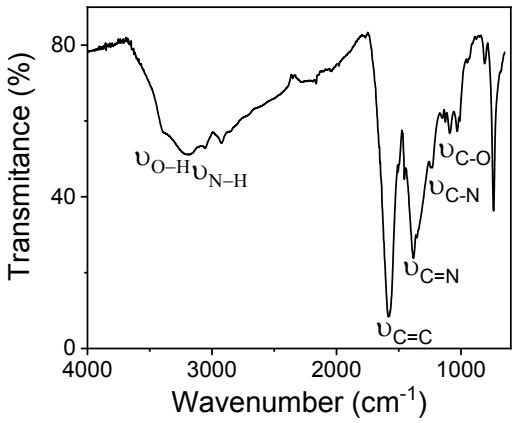

Fig. S1. FT-IR spectra of RCDs.

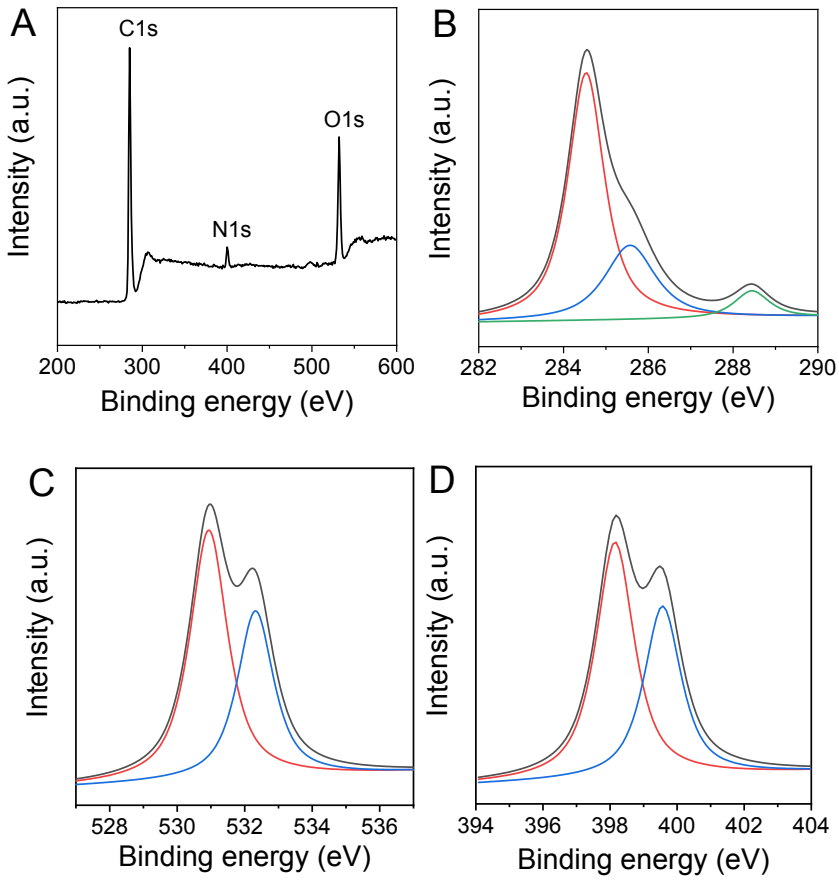

Fig. S2. (A) Survey XPS, (B) C1s (C) O1s and (D) N1s spectra of the RCDs.

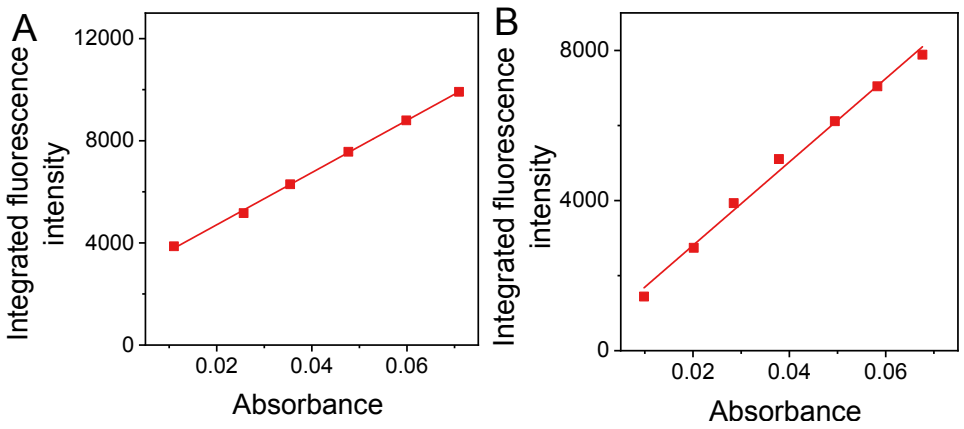

Fig. S3. Integrated fluorescence intensity and absorbance of the rhodamine B (A) and the RCDs (B).

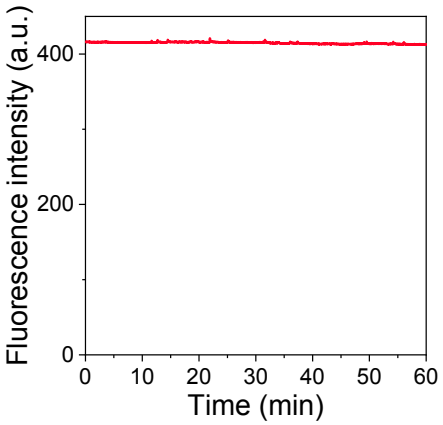

Fig. S4. Fluorescence intensity variation of the RCDs as a function of time under 500 nm light illumination.

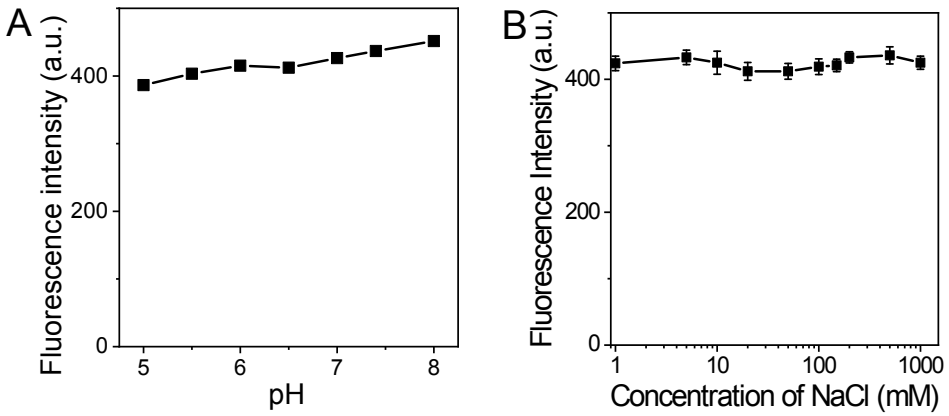

Fig. S5. (A) pH-dependent fluorescence intensity when pH is switched between 5 and 8. (B) Fluorescence intensities of RCDs in 100 mM pH 7.4 PBS after adding various concentrations of NaCl solutions.

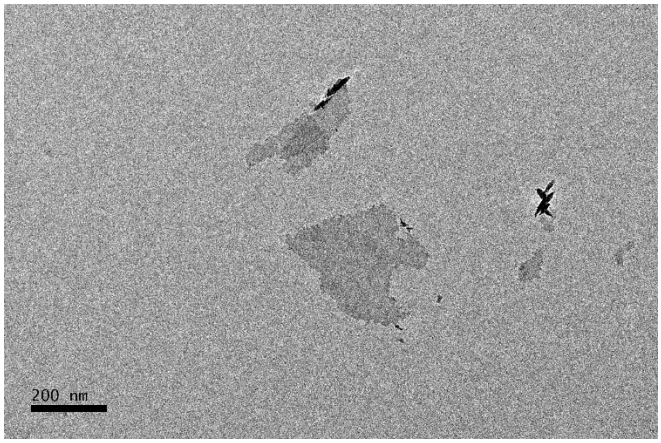

Fig. S6. TEM of Ti_3C_2 nanosheets.

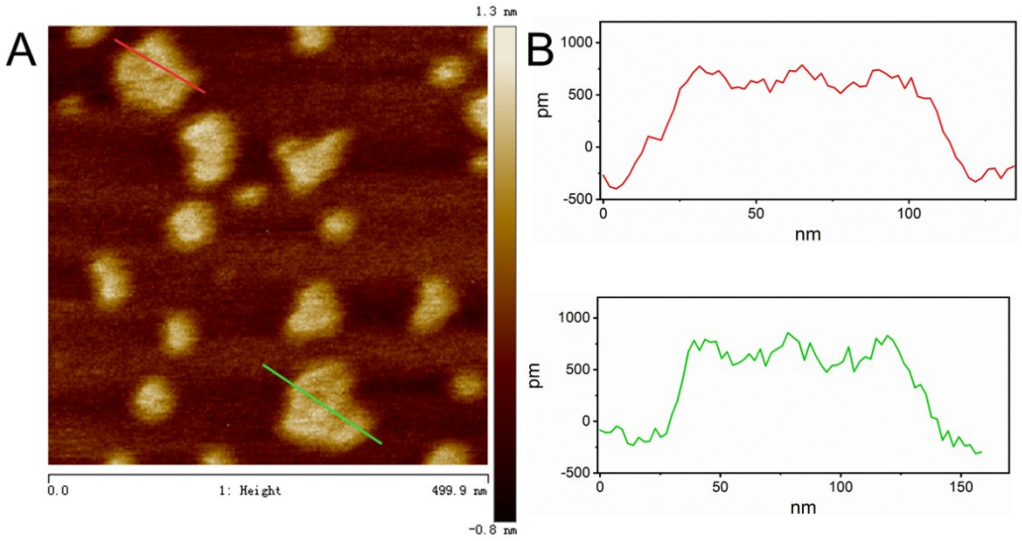

Fig. S7. (A) AFM topography image of Ti_3C_2 nanosheets and (B) height profile along the line in the topographic image.

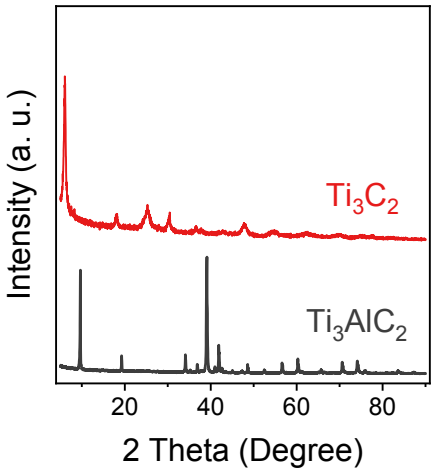

Fig. S8. XRD patterns of Ti_3AlC_2 and Ti_3C_2 nanosheets.

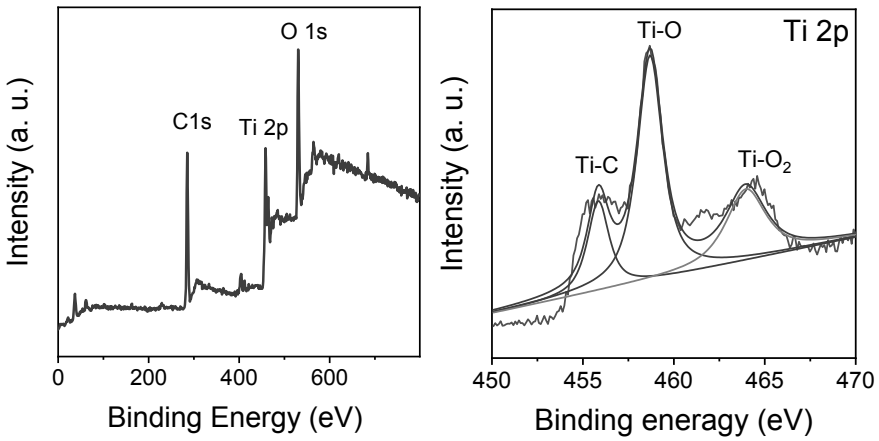

Fig. S9. (A) Survey XPS, and (B) Ti 2p spectra of the Ti_3C_2 nanosheets.

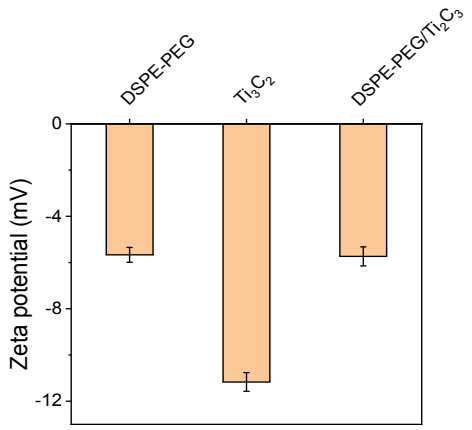

Fig. S9. Surface zeta potential of DSPE-PEG, Ti_2C_3 nanosheets, and DSPE-PEG/Ti_2C_3. Bars represent means ± SD (n = 3).

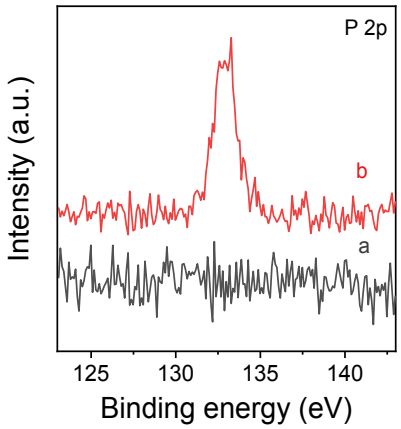

Fig. S10. XPS P 2p spectra of the Ti_3C_2 nanosheets (curve a) and DSPE-PEG/Ti_3C_2 (curve b).

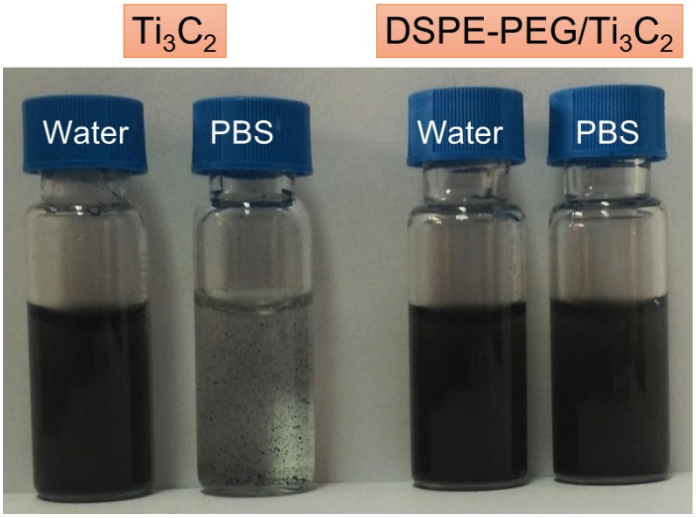

Fig. S11. Photos of Ti_3C_2 and DSPE-PEG/Ti_2C_3 in water and PBS.

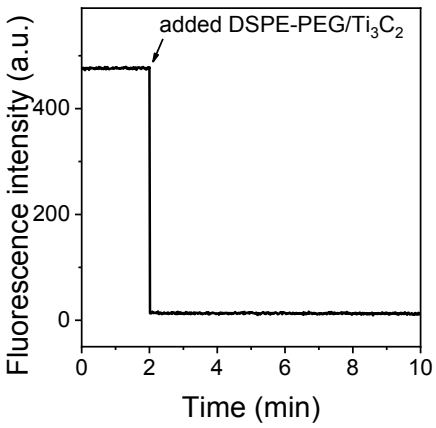

Fig. S12. Time-dependent fluorescence changes of RCDs (5μg mL^{-1}) after the addition of DSPE/PEG-Ti_3C_2 (50 μg mL^{-1}) at room temperature.

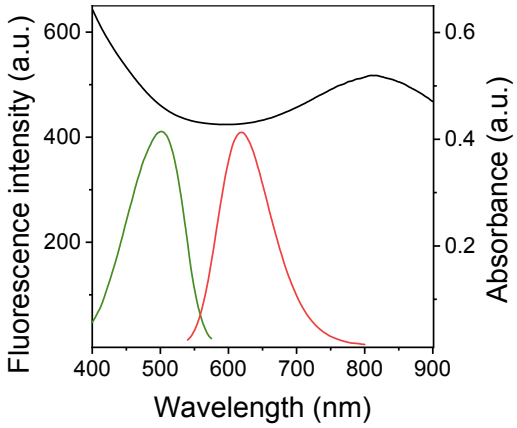

Fig. S13. UV-vis spectra of DSPE-PEG/Ti_3C_2 (50 μg mL^{-1}) and fluorescence excitation and emission spectra of RCDs (5 μg mL^{-1}).

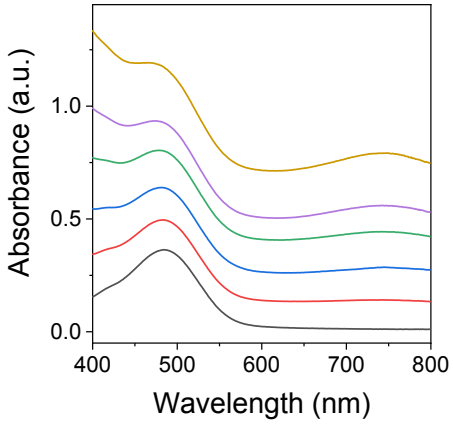

Fig. S14. UV-vis spectra of RCDs (5 μg mL^{-1}) upon addition of various concentrations of DSPE-PEG/Ti_3C_2 (from bottom to top: 0, 5, 10, 15, 20, and 25 μg mL^{-1})

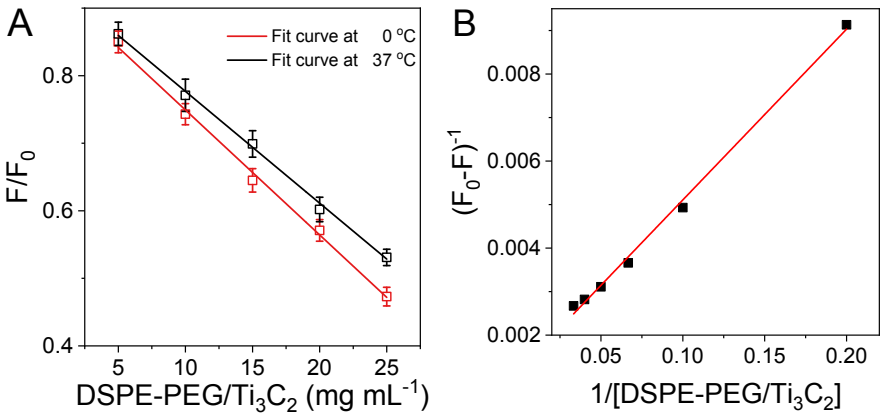

Fig. S15. (A) Fluorescence responses of RCDs in the presence of different concentration DSPE-PEG/Ti_3C_2 at 0 °C and 37 °C. F_0 and F are the fluorescence intensity of RCDs in the absence and presence of DSPE-PEG/Ti_3C_2, respectively. (B) Lineweaver-Burke plot of fluorescence quenching of RCDs by DSPE-PEG/Ti_3C_2. The concentration of RCDs is 5 μg mL^{-1}.

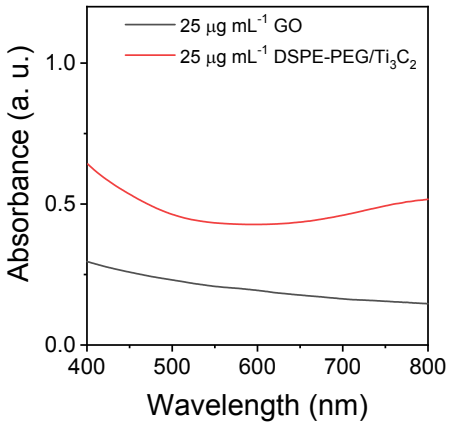

Figure S16. UV-vis spectra of GO and DSPE-PEG/Ti_3C_2.

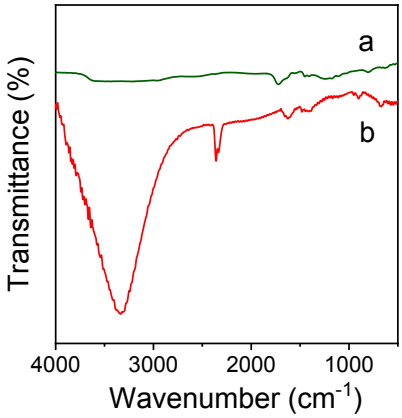

Fig. S17. The FTIR spectra of Ti_3C_2 (curve a) and H_2O_2 treated Ti_3C_2 (curve b).

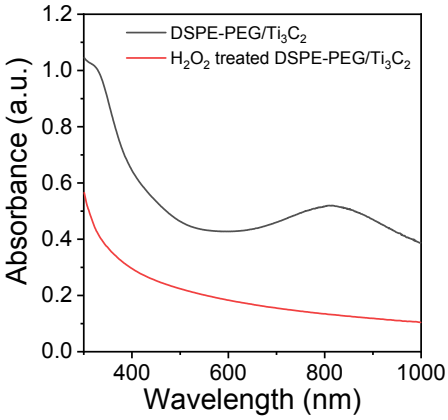

Fig. S18. (A) The UV-vis spectra of DSPE-PEG/Ti_3C_2 (25 μg mL^{-1}) and H_2O_2 (10 mM) treated DSPE-PEG/Ti_3C_2.

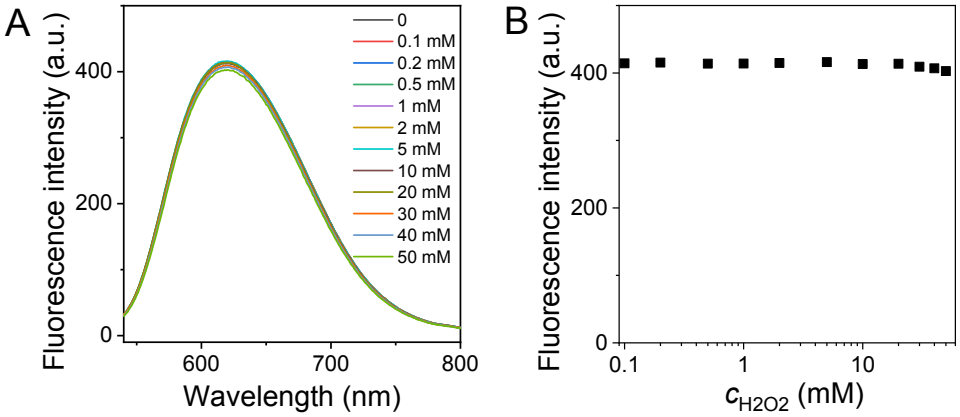

Fig. S19. (A) Fluorescence spectra of RCDs toward different concentrations of H_2O_2. (B) Influence of H_2O_2 concentration on the fluorescence intensity of RCDs.

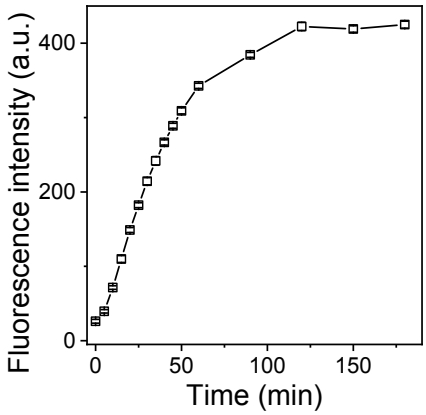

Fig. S20. The effects of incubation time on the fluorescence intensity of DSPE-PEG/Ti_3C_2/RCDs and H_2O_2 (10 mM).

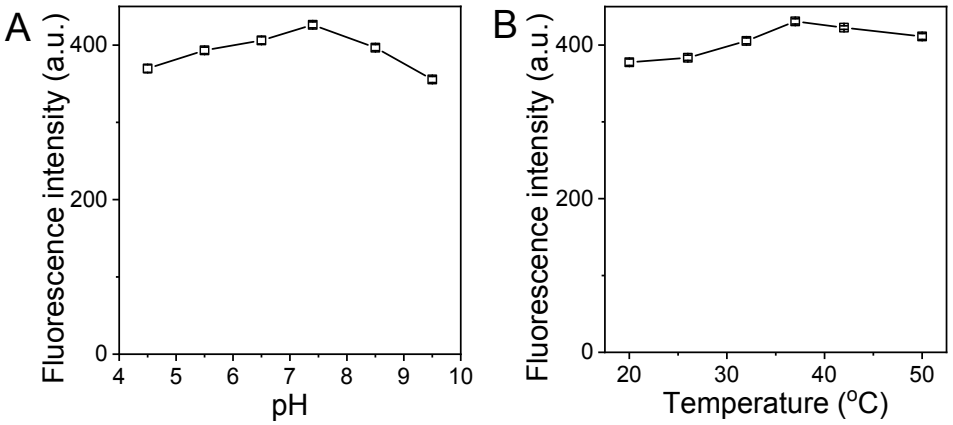

Fig. S21. Effects of pH value (A) and temperature (B) on the fluorescence intensity of DSPE-PEG/Ti_3C_2/RCDs nanosystem in the presence of 10 mM H_2O_2.

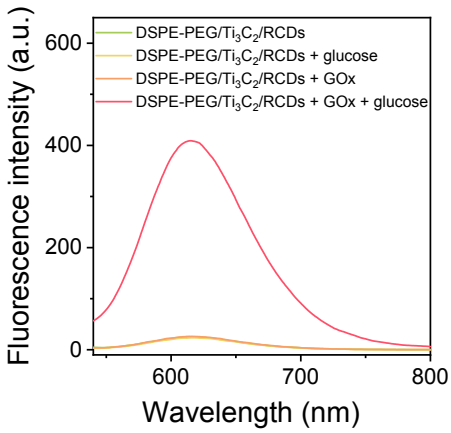

Fig. S22. Fluorescence response of DSPE-PEG/Ti_3C_2/RCDs nanosystem, DSPE-PEG/Ti_3C_2/RCDs nanosystem with glucose (30 mM), GOx (0.05 mg mL^{-1}), and with the reaction products of glucose (30 mM) and GOx (0.05 mg mL^{-1}).

References

(1) Y. Liu, W. Duan, W. Song, J. Liu, C. Ren, J. Wu, D. Liu and H. Chen, ACS Appl. Mater. Interfaces, 2017, **9**, 12663-12672.

(2) W. Li, S. Wu, H. Zhang, X. Zhang, J. Zhuang, C. Hu, Y. Liu, B. Lei, L. Ma and X. Wang, Adv. Funct. Mater., 2018, **28**, 1804004.

(3) H. Ding, Y. Ji, J.-S. Wei, Q.-Y. Gao, Z.-Y. Zhou and H.-M. Xiong, J. Mater. Chem. B, 2017, **5**, 5272-5277.

(4) J. Liu, D. Li, K. Zhang, M. Yang, H. Sun and B. Yang, Small, 2018, **14**, 1703919.

(5) Z. Wang, F. Yuan, X. Li, Y. Li, H. Zhong, L. Fan and S. Yang, Adv. Mater., 2017, **29**, 1702910.

(6) M. Yu, K. Zhao, X. Zhu, S. Tang, Z. Nie, Y. Huang, P. Zhao and S. Yao, Biosens. Bioelectron., 2017, **95**, 41-47.

(7) X. Shan, L.Chai, J. Ma, Z. Qian, J. Chen and H. Feng, Analyst, 2014, **139**, 2322-2325.

(8) H. Zheng, R. Su, Z. Gao, W. Qi, R. Huang, L. Wang and Z. He, Anal. Methods, 2014, **6**, 6352-6357.

(9) X. Wu, F. Tian, W. Wang, J. Chen, M. Wu, and J. X. Zhao, J. Mater. Chem. C, 2013, **1**, 4676-4684.

(10) L. Su, L. Yang, Q. Sun, T. Zhao, B. Liu, C. Jiang and Z. Zhang, New J. Chem., 2018, **42**, 6867-6872.

(11) Y. Tang, Q. Yang, T. Wu, L. Liu, Y. Ding and B. Yu, Langmuir, 2014, **30**, 6324-6330.

(12) L. L. Wang, J. Qiao, H. H. Liu, J. Hao, L. Qi, X. P. Zhou, Z. X. D. Li, Nie and L. Q. Mao, Anal. Chem., 2014, **86**, 9758-9764.

(13) L. Zhang, F. Su, S. Buizer, X. Kong, F. Lee, K. Day, Y. Tian and D. R. Meldrum, Chem. Commun., 2014, **50**, 6920-6922.

(14) Y. Tang, Q. Yang, T. Wu, L. Liu, Y. Ding and B. Yu, Langmuir 2014, **30**, 6324-6330.